Structural Engineering and Mechanics, Vol. 18, No. 3 (2004) 315-330
DOI: http://dx.doi.org/10.12989/sem.2004.18.3.315

Interface characteristics of RC beams strengthened with FRP plate

Minglan Peng† and Zhifei Shi‡

School of Civil Engineering, Beijing Jiaotong University, Beijing 100044, China

(Received June 19, 2003, Accepted April 22, 2004)

Abstract. A four-point bending RC beam strengthened with FRP plate is investigated based on the theory of elasticity. Taking the adhesive layer into account but ignoring some secondary parameters, the analytical solutions of the normal stress and shear stress on concrete-adhesive interface are obtained and discussed. Besides, the pure bending region of the beam is analyzed and the ultimate load of the beam is predicted. The results obtained in the present paper agree very well with both the results of FEM and the experimental findings.

Key words: FRP plate; adhesive layer; reinforced beam; ultimate load; composites.

1. Introduction

Due to many advantages, such as low weight, high strength and good durability, Fiber-Reinforced Polymer (FRP) composite materials have been extensively used for repairing and/or strengthening damaged structures (Shahawy *et al*. 1996, Ritchie *et al.* 1991). The behavior of the strengthened structures depends not only on the individual materials, but also on the properties of the interfaces, namely, the concrete-adhesive and FRP/plate-adhesive interfaces. Till now, a great number of investigations have been made considering flexural members strengthened by FRP sheets or plate. In these investigations, in order to find the distributions of stresses in the strengthened beam, the shear-lag model (Zheng 1999) and the contained adhesive layer model (OuYang and Qian 2000, Roberts 1989) are introduced and modified. Besides, some experimental studies have also been conducted, such as modeling the global behavior of a beam (Arduini and Nanni 1997, Arduini *et al.* 1997), single-face shear experiment (Chajes *et al.* 1996), peel-off experiment (Xie *et al.* 1995), double-face shear experiment (Nakaba *et al*. 2001) and effects of temperatures (Tommaso *et al*. 2001), etc. Despite a considerable number of theoretical works treating this subject, a few research papers are identified that provide a simple analytical process and expression that are capable of producing results in good agreement with results obtained from both numerical analysis and experimental findings.

Based on the theory of elasticity, a four-point bending RC beam strengthened with FRP plate is studied in the present paper. Under the consideration of equilibrium equations and compatibility

† Graduate Student
‡ Professor

equations for concrete, adhesive layer and the FRP plate, respectively, the analytical solutions for evaluating the normal stress and shear stress on the interfaces near the FRP plate's end are obtained. By ignoring some secondary parameters and making some suitable simplification, the obtained solutions become very simple yet can produce reasonable accuracy. Finally the pure bending region of the beam is analyzed and the ultimate load of the beam is predicted. The results obtained in the present paper agree very well with those obtained by FEM and experimental analysis. The present investigation provides a very simple analytical method for the types of strengthened engineering structures considered.

2. The normal stress and shear stress on the interface

A four-point bending, simply supported beam is considered in the present paper. The Cartesian coordinate system *x-y* is introduced as shown in Fig. 1. Without loss of generality, the following assumptions are introduced in this section: (A) the concrete and adhesive as well as the FRP plate are linearly elastic, isotropic and small deformation; (B) the concrete and FRP plate are perfectly bonded; (C) the distribution of stresses in the cross sections of adhesive layer and FRP plate is uniform when bending moment is small; (D) no initial cracks are present in the concrete; (E) the plane sections of the strengthened beam before bending remain plane after bending.

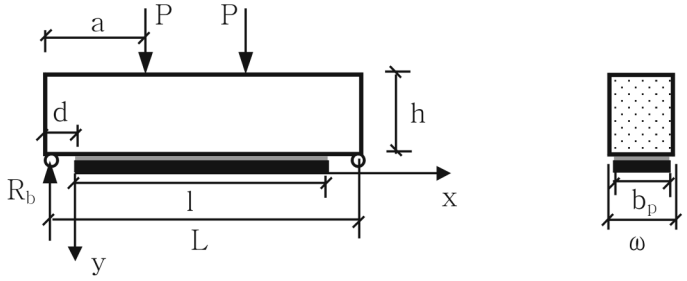

Fig. 1 Schematic of the simply supported FRP reinforced concrete beam

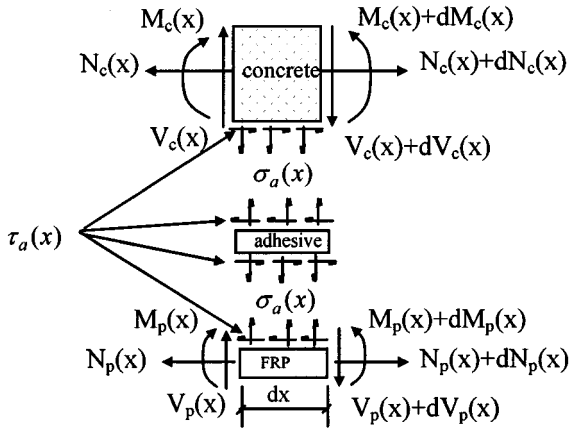

Fig. 2 Equilibrium forces of a small element with length *dx*

Based on these assumptions, the analytical solutions of the normal stress and shear stress on the interface between concrete and the adhesive layer (or between the layer and FRP plate) are discussed first. For the strengthened beam, the distribution of stress near the FRP plate's end changes greatly due to the abrupt change of the beam's stiffness. So peeling type failure often takes place within this section. Based on a small element of length dx as shown in Fig. 2, the equilibrium equations of the element can be presented as follows

$$dN_c(x) = -\tau_a(x)b_p dx \tag{1a}$$

$$dV_c(x) = -\sigma_a(x)b_p dx \tag{1b}$$

$$dM_c(x) = V_c(x)dx - \tau_a(x)b_p y_0 dx \tag{1c}$$

$$dN_p(x) = \tau_a(x)b_p dx \tag{2a}$$

$$dV_p = \sigma_a(x)b_p dx \tag{2b}$$

$$dM_p(x) = V_p(x)dx - \tau_a(x)b_p \frac{t_p}{2} dx \tag{2c}$$

where M_i, N_i and $V_i (i = c, p)$ denote the bending moment, the axial force and the shear force of the corresponding section, respectively. Subscripts a, c and p denote adhesive, concrete and the FRP plate, respectively. In addition b_p and t_p denote the width and thickness of the FRP plate, respectively, and y_0 is the distance from the neutral axis of the FRP plate. Let $\tau_a(x)$ and $\sigma_a(x)$ represent the shear and normal stresses in the adhesive, respectively. When the quantity of the reinforcement and the size of the beam are known, y_0 can be determined.

Based on the theory of elasticity, the shear stress $\tau_a(x)$ can be expressed as

$$\tau_a(x) = \frac{G_a}{t_a}[u_p(x) - u_c(x)] \tag{3}$$

where u_c and u_p denote the horizontal displacement of the low surface of the concrete and the upper surface of the FRP plate, respectively. While G_a and t_a represent the shear modulus and thickness of the adhesive layer, respectively. Further more, $\tau_a(x)$ can also be expressed by strain $\varepsilon_p(x)$ and $\varepsilon_c(x)$ by differentiating Eq. (3)

$$\frac{d\tau_a(x)}{dx} = \frac{G_a}{t_a}[\varepsilon_p(x) - \varepsilon_c(x)] \tag{4}$$

In order to simplify the analysis, the Poisson's effect is ignored in the present paper. Recognizing that the thickness of the FRP plate is relatively small, the effect of bending moment of FRP on $\varepsilon_p(x)$ can also be ignored. So Eq.(4) can be rewritten

$$\frac{d\tau_a(x)}{dx} = \frac{G_a}{t_a}\left[\frac{N_p(x)}{E_p b_p t_p} - \frac{M_c(x)y_0}{E_c I_c} - \frac{N_c(x)}{E_c \omega h}\right] \tag{5}$$

where ω and h represent the width and depth of the concrete beam, respectively, while E_c and E_p represent the elastic modulus of the concrete and FRP plate, respectively.

Differentiating Eq. (5) again and substituting Eq. (1a), Eq. (1c), Eq. (2a) into it, we obtain

$$\frac{d^2\tau_a(x)}{dx^2} = \frac{G_a}{t_a}\left[\frac{1}{E_p t_p} + \frac{b_p}{E_c \omega h} + \frac{b_p y_0^2}{E_c I_c}\right]\tau_a(x) - \frac{G_a y_0}{E_c t_a I_c} V_c(x) \tag{6}$$

Further considering the thickness of the FRP plate is relatively small as compared with the concrete depth, it is assumed that the contribution of the FRP plate to the shear force in the cross section of the beam can be neglected, which means we can take $V_c(x) \approx R_b = P$. Where R_b and P denote the vertical reaction force and the applied load, respectively. So Eq. (6) can be expressed in detail as

$$\frac{d^2\tau_a(x)}{dx^2} = \frac{G_a}{t_a}\left[\frac{1}{E_p t_p} + \frac{b_p}{E_c \omega h} + \frac{b_p y_0^2}{E_c I_c}\right]\tau_a(x) - \frac{G_a y_0}{E_c t_a I_c} P \tag{7}$$

The solution of the above equation is given by

$$\tau_a(x) = C_1 \cosh(\alpha x) + C_2 \sinh(\alpha x) + \eta_0 \tag{8}$$

where $\alpha^2 = \frac{G_a}{t_a}\left[\frac{1}{E_p t_p} + \frac{b_p}{E_c \omega h} + \frac{b_p y_0^2}{E_c I_c}\right]$, $\eta_0 = \frac{G_a y_0 P}{E_c I_c t_a \alpha^2}$. The arbitrary constants C_1 and C_2 will be determined by some appropriate boundary conditions. For the four-point bending beam, it is obvious that the following boundary conditions can be used, i.e., $N_p(x)\big|_{x=0} = N_c(x)\big|_{x=0} = 0$, $M_c(x)\big|_{x=0} = Pd$. On the other hand, in the pure bending region of the beam, the shear stress is equal to zero, i.e., $\tau_a(x) \to 0$. Using these boundary conditions, we can obtain

$$C_1 = \frac{G_a P d y_0}{E_c I_c t_a \alpha}\tanh[\alpha(a-d)] - \frac{\eta_0}{\cosh[\alpha(a-d)]}, \quad C_2 = -\frac{G_a P d y_0}{E_c I_c t_a \alpha} \tag{9}$$

Considering that when $\alpha(a-d) > 10$, the second term in C_1 can be approximated to be zero and $\tanh[\alpha(a-d)]$ to be 1, so we have $C_1 = \frac{G_a P d y_0}{E_c I_c t_a \alpha}$. Then $\tau_a(x)$ can be simplified to $\tau_a(x) = C_1 e^{-\alpha x} + \eta_0$.

It is obvious that the maximum shear stress can be obtained as follows

$$\tau_{a\cdot\max} = \tau_a(0) = C_1 + \eta_0 = \frac{G_a P y_0}{E_c I_c t_a \alpha^2}(d\alpha + 1) \tag{10}$$

Secondly, let's find the distribution of the normal stress. Based on the theory of elasticity, the normal stress can be simply defined as

$$\sigma_a(x) = E_a \frac{\upsilon_p(x) - \upsilon_c(x)}{t_a} \tag{11}$$

where υ_c and υ_p denote the vertical displacement of the concrete and the FRP plate, respectively, E_a and t_a the elastic modulus and thickness of the adhesive. On the other hand, we have the following differential relations

$$\frac{d^2\upsilon_c(x)}{dx^2} = -\frac{M_c(x)}{E_c I_c}, \quad \frac{d^2\upsilon_p(x)}{dx^2} = -\frac{M_p(x)}{E_p I_p} \tag{12}$$

Solving Eq. (11) and Eq. (12) (see Appendix I), the expression of $\sigma_a(x)$ can be obtained as

$$\sigma_a(x) = H_1 e^{-\lambda x}\cos(\lambda x) + H_2 e^{-\lambda x}\sin(\lambda x) - \frac{\alpha\gamma C_1}{\alpha^4 + 4\lambda^4} e^{-\alpha x} \tag{13}$$

where H_1 and H_2 are arbitrary constants and can be determined by using appropriate boundary conditions. Considering $M_p(x)|_{x=0} = V_p(x)|_{x=0} = 0$, $M_c(x)|_{x=0} = Pd$, $V_c(x)|_{x=0} = P$, the following equations can be obtained

$$\left.\frac{d^2 \upsilon_p(x)}{dx^2}\right|_{x=0} = 0, \quad \left.\frac{d^2 \upsilon_c(x)}{dx^2}\right|_{x=0} = -\frac{Pd}{E_c I_c} \tag{14}$$

$$\left.\frac{d^3 \upsilon_p(x)}{dx^3}\right|_{x=0} = \frac{b_p t_p}{2E_p I_p}\tau_{a\cdot\max}, \quad \left.\frac{d^3 \upsilon_c(x)}{dx^3}\right|_{x=0} = -\frac{P}{E_c I_c} + \frac{b_p y_0}{E_c I_c}\tau_{a\cdot\max} \tag{15}$$

Keeping Eq. (11) in mind and by the use of Eq. (14) and Eq. (15) the constants H_1 and H_2 can be determined as $H_1 = \frac{1}{2\lambda^3}\left[\gamma\tau_{a\cdot\max} + \frac{PE_a}{E_c I_c t_a}(1 + d\lambda) + \frac{\alpha^3\gamma C_1}{\alpha^4 + 4\lambda^4}(\lambda - \alpha)\right]$, $H_2 = -\frac{1}{2\lambda^2}\left(\frac{\alpha^3\gamma C_1}{\alpha^4 + 4\lambda^4} + \frac{E_a Pd}{E_c I_c t_a}\right)$. It is also found that $\sigma_a(x)$ gets maximum at $x = 0$

$$\sigma_{a\cdot\max}(x) = \sigma_a(0) = H_1 + \sigma_1(0) \tag{16}$$

where $\sigma_1(0) = -\frac{\alpha\gamma C_1}{\alpha^4 + 4\lambda^4}$

3. Analysis of the pure bending region of the beam

In the failure patterns of a strengthened beam, debonding and fracture usually take place. The former often happens at the end of the FRP plate. In this case, debonding takes place on the interfaces between the concrete and adhesive or adhesive and FRP plate. The latter often happens in the pure bending region $(a - d) \le x \le L - (a + d)$. In this case, cracking of the concrete or fracture of the FRP plate usually takes place. In this section, we focus our attention on the ultimate load of the strengthened beam. In order to simplify the analysis it is assumed that plane sections remain plane and the effect of adhesive layer is ignored because it is very thin. Without loss of generality, the singly under-reinforced rectangular beam is considered and the tensile strength of the concrete is ignored. The schematic of the stress- strain curves for the concrete under compression and for the FRP plate under tension are shown in Fig. 3(a) and Fig. 3(b), respectively.

This means that Rüsch's model and the elastic-perfectly plastic model are used to describe the constitutive relations for the concrete and the FRP plate, respectively. These models can be expressed as follows:

$$\sigma_c = \begin{cases} \sigma_{c0}\left[2\frac{\varepsilon_c}{\varepsilon_0} - \left(\frac{\varepsilon_c}{\varepsilon_0}\right)^2\right] & 0 \le \varepsilon_c \le \varepsilon_0 \\ \sigma_{c0} & \varepsilon_0 < \varepsilon_c \le \varepsilon_{cu} \end{cases} \quad \text{for the concrete under compression} \tag{17}$$

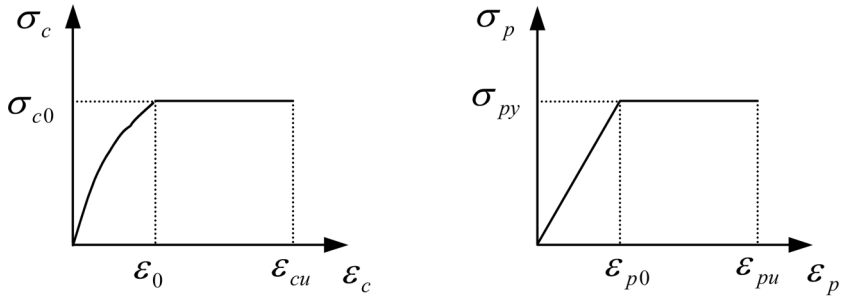

(a) concrete under compression (b) FRP plate under tension

Fig. 3 Schematic of the stress- strain curves for the concrete and the FRP plate

$$\sigma_p = \begin{cases} E_p\varepsilon_p & 0 \le \varepsilon_p \le \varepsilon_{p0} \\ \sigma_{py} & \varepsilon_{p0} < \varepsilon_p \le \varepsilon_{pu} \end{cases} \quad \text{for the FRP plate under tension} \tag{18}$$

For the general case of design for a singly under-reinforced beam failure is gradual. Therefore different failure situations can occur for the beam strengthened with FRP plate depending on the type and amount of the FRP plate provided. So the analytical procedures to find the ultimate load are provided in the following four cases.

Case I: concrete crushing while the FRP plate still being elastic stage

In this case, it is assumed that failure occurs when the strain of the outer face of the compression concrete gets its ultimate strain ε_{cu} (such as 0.0033). The curvature of the neutral axis of the FRP strengthened beam is $\frac{1}{\rho} = \frac{\varepsilon_{cu}}{\hat{y}_0}$. Where $\hat{y}_0$ is the distance from the neutral axis of the beam as shown in Fig. 4. The distance from the neutral axis to the elastic face of the compression concrete can be obtained as $y_c = \frac{\varepsilon_0}{\varepsilon_{cu}}\hat{y}_0$. Where ε_0 (usually taken as 0.002) is the strain of the compression concrete at which the stress of concrete remains a constant. In this case the tensile steels have not reached yield

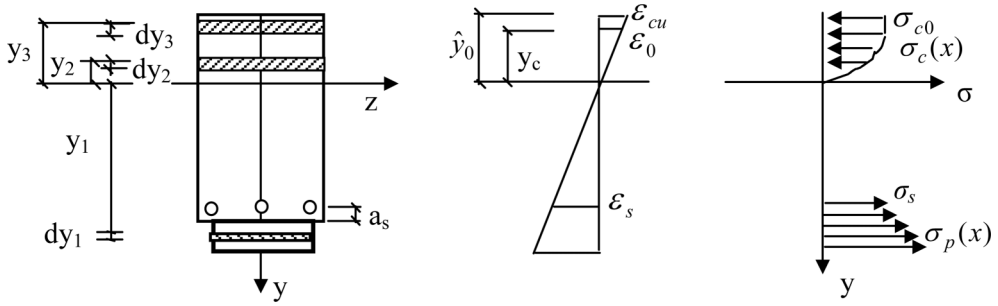

Fig. 4 Schematic of the pure bending section when concrete crushing and the FRP plate still being elastic

and its strain can be obtained as $\varepsilon_s = \frac{\varepsilon_{cu}}{\hat{y}_0}(h-\hat{y}_0-a_s)$, where a_s is the thickness of the protective layer of the tensile steels.

In this region, there is no longitudinal tensile force at any cross section, which means

$$\int_{-\hat{y}_0}^{-\frac{\varepsilon_0}{\varepsilon_{cu}}\hat{y}_0}\sigma_{c0}\omega dy_3+\int_{-\frac{\varepsilon_0}{\varepsilon_{cu}}\hat{y}_0}^{0}\sigma_{c0}\omega\left[\frac{2\varepsilon_{cu}}{\varepsilon_0\hat{y}_0}y_2-\left(\frac{\varepsilon_{cu}y_2}{\varepsilon_0\hat{y}_0}\right)^2\right]dy_2$$

$$=E_sA_s\frac{\varepsilon_{cu}}{\hat{y}_0}(h-\hat{y}_0-a_s)+\int_{h-\hat{y}_0}^{h-\hat{y}_0+t_p}E_p\frac{\varepsilon_{cu}}{\hat{y}_0}y_1b_pdy_1 \tag{19}$$

where y_1, y_2 and y_3 are the distances as shown in Fig. 4; E_s and A_s denote the elastic modulus and total area of the tensile steels, respectively. The position of the neutral axis of the beam is determined as

$$\hat{y}_0=\frac{-b_1+\sqrt{b_1^2-4a_1c_1}}{2a_1} \tag{20}$$

where

$$a_1=2\sigma_{c0}\omega\left(1-\frac{\varepsilon_0}{3\varepsilon_{cu}}\right),\quad b_1=2(E_sA_s\varepsilon_{cu}+E_pA_p\varepsilon_{cu})$$

$$c_1=-[2E_sA_s\varepsilon_{cu}(h-a_s)+E_pA_p\varepsilon_{cu}(2h+t_p)] \tag{21}$$

The moment equilibrium equation of the pure bending section can be expressed as

$$\int_{-\hat{y}_0}^{-\frac{\varepsilon_0}{\varepsilon_{cu}}\hat{y}_0}\sigma_{c0}\omega y_3dy_3+\int_{-\frac{\varepsilon_0}{\varepsilon_{cu}}\hat{y}_0}^{0}\sigma_{c0}\omega\left[\frac{2\varepsilon_{cu}}{\varepsilon_0\hat{y}_0}y_2-\left(\frac{\varepsilon_{cu}y_2}{\varepsilon_0\hat{y}_0}\right)^2\right]y_2dy_2$$

$$+E_sA_s\frac{\varepsilon_{cu}}{\hat{y}_0}(h-\hat{y}_0-a_s)^2+\int_{h-\hat{y}_0}^{h-\hat{y}_0+t_p}E_p\frac{\varepsilon_{cu}}{\hat{y}_0}y_1^2b_pdy_1=Pa \tag{22}$$

Keeping Eq. (20) in mind, the ultimate load of the strengthened beam in case one can be obtained as:

$$P=\frac{1}{a}\left\{\left(\frac{17}{12}\frac{\varepsilon_0^2}{\varepsilon_{cu}^2}-\frac{1}{2}\right)\hat{y}_0^2+E_sA_s\frac{\varepsilon_{cu}}{\hat{y}_0}(h-\hat{y}_0-a_s)^2+E_pb_p\frac{\varepsilon_{cu}}{3\hat{y}_0}[(h-\hat{y}_0+t_p)^3-(h-\hat{y}_0)^3]\right\} \tag{23}$$

Case II: concrete crushing while some of the FRP plate yielding

In this case, some of the FRP plate has reached yield and continues yielding before the concrete fails at the ultimate load. Using ε_{p0} to denote the strain of FRP plate when its stress gets yield stress σ_{py}, the distance from the yield point in the FRP plate to the neutral axis can be obtained as $y_p=\frac{\varepsilon_{p0}}{\varepsilon_{cu}}\hat{y}_0$.

The analytical model in this case is shown in Fig. 5.

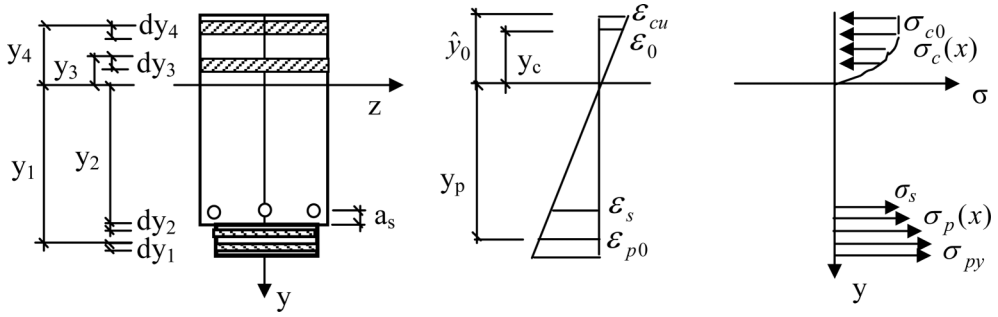

Fig. 5 Schematic of the pure bending section when concrete crushing and some of the FRP plate has reached yield

In a similar way, the position of the neutral axis of the beam can be determined by the consideration of the longitudinal force equilibrium of the beam

$$\hat{y}_0 = \frac{-b_2 + \sqrt{b_2^2 - 4a_2c_2}}{2a_2} \tag{24}$$

where

$$a_2 = \left[E_p b_p \varepsilon_{cu}\left(\frac{\varepsilon_{p0}^2}{\varepsilon_{cu}^2} - 1\right) - 2\sigma_{c0}\omega\left(1 - \frac{\varepsilon_0}{3\varepsilon_{cu}}\right) - 2\sigma_{py}b_p\left(1 + \frac{\varepsilon_{p0}}{\varepsilon_{cu}}\right)\right]$$

$$b_2 = [2\sigma_{py}b_p(h + t_p) + 2E_p b_p h\varepsilon_{cu} - 2E_s A_s \varepsilon_{cu}], \quad c_2 = 2E_s A_s \varepsilon_{cu}(h - a_s) - E_p b_p \varepsilon_{cu} h^2 \tag{25}$$

Besides, the moment equilibrium equation can be written as follows

$$\int_{-\hat{y}_0}^{-\frac{\varepsilon_0}{\varepsilon_{cu}}\hat{y}_0} \sigma_{c0}\omega y_4 dy_4 + \int_{-\frac{\varepsilon_0}{\varepsilon_{cu}}\hat{y}_0}^{0} \sigma_{c0}\omega\left[\frac{2\varepsilon_{cu}}{\varepsilon_0\hat{y}_0}y_3 - \left(\frac{\varepsilon_{cu}y_3}{\varepsilon_0\hat{y}_0}\right)^2\right]y_3 dy_3 + E_s A_s \frac{\varepsilon_{cu}}{\hat{y}_0}(h - \hat{y}_0 - a_s)^2$$
$$+ \int_{h-y_0}^{\frac{\varepsilon_{p0}}{\varepsilon_{cu}}\hat{y}_0} E_p \frac{\varepsilon_{cu}}{\hat{y}_0} y_2^2 b_p dy_2 + \int_{\frac{\varepsilon_{p0}}{\varepsilon_{cu}}\hat{y}_0}^{h-\hat{y}_0+t_p} \sigma_{py} b_p y_1 dy_1 = Pa \tag{26}$$

So we can find the ultimate load of the strengthened beam in this case as follows

$$P = \frac{E_p b_p \varepsilon_{cu}}{3a\hat{y}_0}\left[\left(1 + \frac{\varepsilon_{p0}^3}{\varepsilon_{cu}^3}\right)\hat{y}_0^3 + 3h^2\hat{y}_0 - 3h\hat{y}_0 - h^3\right] + \frac{1}{2a}\sigma_{py}b_p\left[(h + t_p - \hat{y}_0)^2 - \frac{\varepsilon_{p0}^2}{\varepsilon_{cu}^2}\hat{y}_0^2\right]$$
$$+ \frac{1}{a}\left(\frac{17}{12}\frac{\varepsilon_0^2}{\varepsilon_{cu}^2} - \frac{1}{2}\right)\sigma_{c0}\omega\hat{y}_0^2 + E_s A_s \frac{\varepsilon_{cu}}{a\hat{y}_0}(h - \hat{y}_0 - a_s)^2 \tag{27}$$

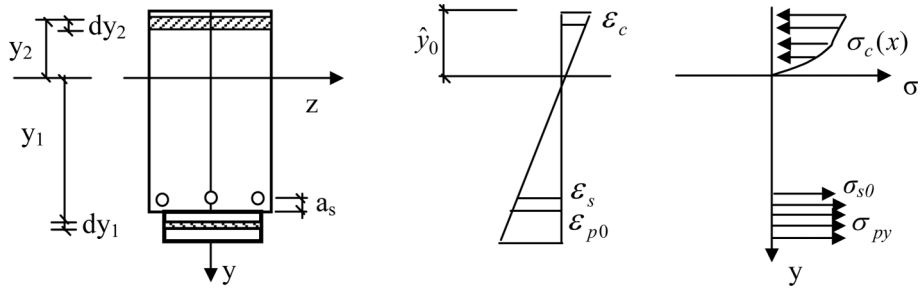

Fig. 6 Schematic of the pure bending section when the FRP plate rupturing and the concrete still being elastic

Case III: the FRP plate rupturing while the whole concrete still being elastic

In this case, it is assumed that rupture happens when the whole cross section of the FRP plate has reached yield. At the same time, the reinforcement has reached yield too and the yield stress of the tensile steels is denoted by σ_{s0}. The whole concrete in compression is yet being elastic. The curvature of the neutral axis of the FRP strengthened beam can be found as $\frac{1}{\rho} = \frac{\varepsilon_{p0}}{h-\hat{y}_0}$. The analytical model in this case is shown in Fig. 6.

The longitudinal force equilibrium equation of the beam can be found as follows

$$\sigma_{s0}A_s + \sigma_{py}b_pt_p = \int_{-\hat{y}_0}^{0}\sigma_{c0}\omega\left[\frac{2\varepsilon_{p0}}{\varepsilon_0}\frac{y_2}{h-\hat{y}_0} - \left(\frac{\varepsilon_{p0}}{\varepsilon_0}\frac{y_2}{h-\hat{y}_0}\right)^2\right]dy_2 \tag{28}$$

The position of the neutral axis of the beam in this case can be determined as

$$\hat{y}_0 = -\frac{a_3}{3} + \sqrt[3]{-\frac{q}{2} + \sqrt{\frac{q^2}{4} + \frac{p^3}{27}}} + \sqrt[3]{-\frac{q}{2} - \sqrt{\frac{q^2}{4} + \frac{p^3}{27}}} \tag{29}$$

where

$$a_3 = \left(\frac{\varepsilon_{p0}}{\varepsilon_0}h + \bar{c}_3\right)\Big/\bar{a}_3, \quad b_3 = -\frac{2\bar{c}_3h}{\bar{a}_3}, \quad c_3 = \frac{\bar{c}_3h^2}{\bar{a}_3}$$
$$\bar{a}_3 = \frac{1}{3}\left(\frac{\varepsilon_{p0}}{\varepsilon_0}\right)^2 - \frac{\varepsilon_{p0}}{\varepsilon_0}, \quad \bar{c}_3 = \frac{\sigma_{s0}A_s + \sigma_{py}b_pt_p}{\sigma_{c0}\omega}$$
$$p = b_3 - \frac{1}{3}a_3^2, \quad q = \frac{2}{27}a_3^3 - \frac{a_3b_3}{3} + c_3 \tag{30}$$

The moment equilibrium equation of the pure bending section can be expressed as

$$\int_{-\hat{y}_0}^{0}\sigma_{c0}\omega\left[\frac{2\varepsilon_{p0}}{\varepsilon_0}\frac{y_2}{h-\hat{y}_0} - \left(\frac{\varepsilon_{p0}}{\varepsilon_0}\frac{y_2}{h-\hat{y}_0}\right)^2\right]y_2dy_2 + \sigma_{s0}A_s(h-\hat{y}_0-a_s) + \sigma_{py}b_pt_p\left(h-\hat{y}_0+\frac{t_p}{2}\right) = Pa \tag{31}$$

Keeping Eq. (29) in mind, the ultimate load of the strengthened beam in this case can be found as

$$P = \frac{1}{a}\left\{\sigma_{c0}\omega\left[\frac{2\varepsilon_{p0}}{3\varepsilon_0}\frac{\hat{y}_0^3}{h-\hat{y}_0} + \left(\frac{\varepsilon_{p0}}{2\varepsilon_0}\frac{\hat{y}_0^2}{h-\hat{y}_0}\right)^2\right] + \sigma_{s0}A_s(h-\hat{y}_0-a_s) + \sigma_{py}b_pt_p\left(h-\hat{y}_0+\frac{t_p}{2}\right)\right\} \tag{32}$$

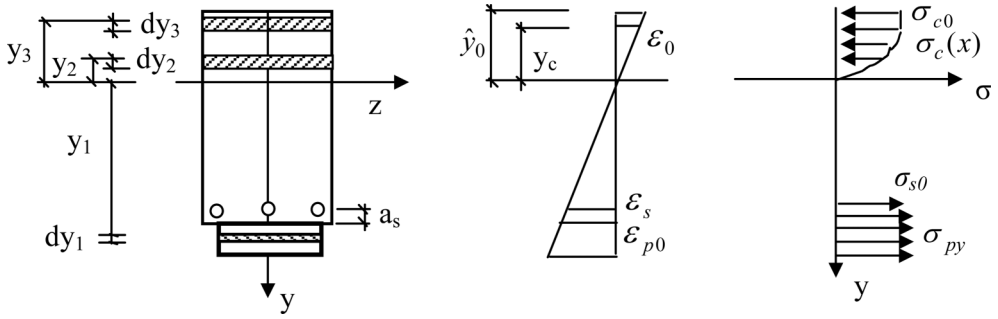

Fig. 7 Schematic of the pure bending section when the FRP plate rupturing and some of the concrete yielding

Case IV: the FRP plate rupturing while some of the concrete yielding

In this case, it is assumed that some of the concrete has reached yield when the FRP plate is fractured. At the same time, the stress in tensile steel gets σ_{s0}. The curvature of the neutral axis of the FRP strengthened beam can be found as $\frac{1}{\rho} = \frac{\varepsilon_{p0}}{h-\hat{y}_0}$. The height of the un-yield concrete can be determined as $y_c = \frac{\varepsilon_0}{\varepsilon_{p0}}(h-\hat{y}_0)$. The analytical model in this case is shown in Fig. 7.

In a similar way to case three the longitudinal force equilibrium equation of the beam can be found as

$$\int_{-\hat{y}_0}^{-\frac{\varepsilon_0}{\varepsilon_{p0}}(h-\hat{y}_0)} \sigma_{c0}\omega dy_3 + \int_{-\frac{\varepsilon_0}{\varepsilon_{p0}}(h-\hat{y}_0)}^{0} \sigma_{c0}\omega\left[\frac{2\varepsilon_{p0}}{\varepsilon_0}\frac{y_2}{h-\hat{y}_0} - \left(\frac{\varepsilon_{p0}}{\varepsilon_0}\frac{y_2}{h-\hat{y}_0}\right)^2\right]dy_2 = \sigma_{s0}A_s + \sigma_{py}b_p t_p \tag{33}$$

The position of the neutral axis of the beam in this case can be determined as

$$\hat{y}_0 = \frac{3(\sigma_{s0}A_s + \sigma_{py}b_p t_p)\varepsilon_{p0} + 7\varepsilon_0\sigma_{c0}\omega h}{\sigma_{c0}\omega(3\varepsilon_{p0} + 7\varepsilon_0)} \tag{34}$$

The moment equilibrium equation of the pure bending section can be written as

$$\int_{-\hat{y}_0}^{-\frac{\varepsilon_0}{\varepsilon_{p0}}(h-\hat{y}_0)} \sigma_{c0}\omega y_3 dy_3 + \int_{-\frac{\varepsilon_0}{\varepsilon_{p0}}(h-\hat{y}_0)}^{0} \sigma_{c0}\omega\left[\frac{2\varepsilon_{p0}}{\varepsilon_0}\frac{y_2}{h-\hat{y}_0} - \left(\frac{\varepsilon_{p0}}{\varepsilon_0}\frac{y_2}{h-\hat{y}_0}\right)^2\right]y_2 dy_2 + \sigma_{s0}A_s(h-\hat{y}_0-a_s) + \sigma_{py}b_p t_p\left(h-\hat{y}_0+\frac{t_p}{2}\right) = Pa \tag{35}$$

Thus the ultimate load of the strengthened beam in this case can be found as:

$$P = \frac{\sigma_{c0}\omega}{2a}\left[\frac{17\varepsilon_0^2}{6\varepsilon_{p0}^2}(h-\hat{y}_0)^2 - \hat{y}_0^2\right] + \frac{\sigma_{s0}A_s}{a}(h-\hat{y}_0-a_s) + \frac{\sigma_{py}b_p t_p}{a}\left(h-\hat{y}_0+\frac{t_p}{2}\right) \tag{36}$$

4. Comparison between numerical and experimental results and theoretical calculations

The theoretical results presented in the present paper are compared with the results obtained from both numerical analysis and experimental finding (Malek *et al*. 1998, OuYang and Huang 2002). Firstly, in order to compare with the results obtained from FEM analysis, the details of the beam used in (Malek *et al.* 1998) are listed as follows: $L \times \omega \times h = 4575 \times 205 \times 455$ (mm^3), $l \times b_p \times t_p = 4265 \times 152 \times 6$ (mm^3), $d = 155$ mm, $t_a = 1.5$ mm, $a = 1982.5$ mm, $P = 100$ kN, $E_c = 27.990$ GPa, $E_p = 37.230$ GPa, $E_a = 0.814$ GPa, $G_a = 0.297$ GPa, $y_0 = 227.5$ mm. Based on these data and Eq. (8) and Eq. (13), the distributions of shear stress $\tau_a(x)$ and normal stress $\sigma_a(x)$ are obtained and plotted in Fig. 8 and Fig. 9, respectively. The numerical results of $\tau_a(x)$ and $\sigma_a(x)$ obtained in (Malek *et al.* 1998) are also plotted in Fig. 8 and Fig. 9. It is easily found that the results obtained in the present paper agree well with that given by the numerical analysis.

Secondly, let's compare the results obtained in the present paper with the experimental findings (OuYang and Huang 2002). The material properties and geometrical parameters of the FRP reinforced beams used in the experiment (OuYang and Huang 2002) are listed in Table 1.

For the structural need, every tested beam is reinforced by 2ϕ 12 in the tensile section. It is found in the experiments (OuYang and Huang 2002) that debonding takes place between the concrete and adhesive or adhesive and GFRP plate in these beams listed in Table 1. Now let's calculate the maximum principal stress σ_1 at the interface between concrete and adhesive layer in the GFRP plate's end. When d is small, the bending stress in the concrete near the GFRP plate's end is small too. So the influence of the bending stress on σ_1 can be neglected and we have:

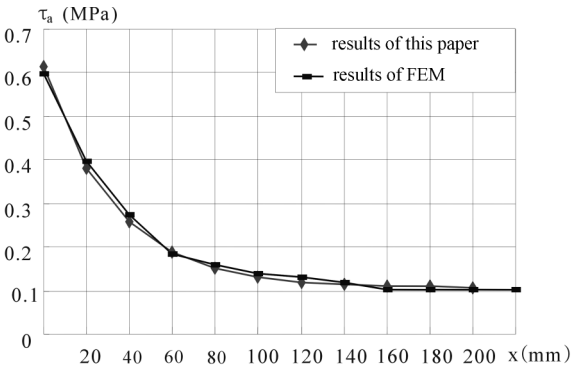

Fig. 8 Distribution of shear stress along the interface

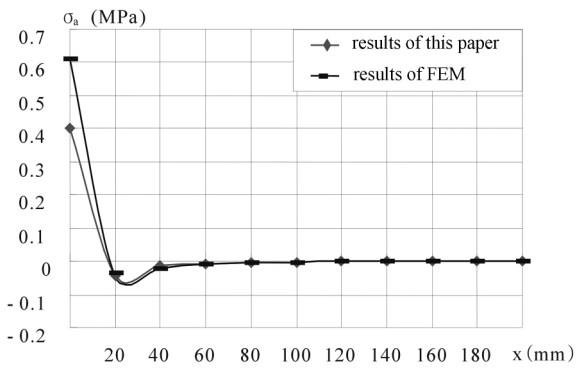

Fig. 9 Distribution of normal stress along the interface

Table 1 Constants of the FRP reinforced beams (notes f_{tk} - the tensile strength of the concrete.)

No. of beams	t_p (mm)	d (mm)	Other material properties and geometrical parameters
ML02	2	100	$L \times \omega \times h = 1400 \times 100 \times 160$ (mm^3);
ML03	3	100	$E_c = 24$ GPa, $f_{tk} = 1.1$ MPa; $E_p = 11$ GPa, $b_p = 100$ mm;
ML04	1	200	$t_a = 0.4$ mm, $E_a = 5.7$ GPa, $G_a = 2.05$ GPa

Table 2 The anchorage elastic load obtained from different ways (with *----- present paper, others ----- (OuYang and Huang 2002))

Serial number	Calculated value * (kN)	Calculated value (kN)	$\tau_{a\cdot\max}$ * (MPa)	$\tau_{a\cdot\max}$ (MPa)	$\sigma_{a\cdot\max}$ * (MPa)	$\sigma_{a\cdot\max}$ (MPa)	Experimental value (kN)	σ_1 (MPa)	Δ* (%)	Δ (%)
ML02	12.43	12.30	0.605	0.607	0.767	0.765	15.0	1.10	17.1	18.0
ML03	9.69	9.65	0.580	0.583	0.794	0.790	10.0	1.10	3.1	3.5
ML04	9.53	9.83	0.650	0.650	0.716	0.717	10.0	1.10	4.7	6.2

notes Δ^*= (calculated value * -experimental value)/experimental value; Δ = (calculated value -experimental value)/experimental value. Δ^* and Δ represent the errors of the present paper and (OuYang and Huang 2002), respectively.

$$\sigma_1 = \frac{1}{2}\sigma_{a\cdot\max} + \frac{1}{2}\sqrt{\sigma_{a\cdot\max}^2 + 4\tau_{a\cdot\max}^2} \tag{37}$$

When σ_1 gets to the tensile strength, the concrete near the GFRP plate's end will crack. Then the applied load is usually defined as the anchorage elastic load. Table 2 gives the anchorage elastic load calculated based on Eq. (10), Eq. (16) and Eq. (37). Listed in Table 2 also gives the experimental findings and another analytical results based on different model (OuYang and Huang 2002). The results obtained in are simplified from the formulas of the bonded beam subjected to a linearly distributed loading at the upper surface. In the analysis (OuYang and Huang 2002), a lot of unknown parameters should be determined and the analytical process is very complicated. It is also found that the predicted values given by the present analysis also agree well with the experimental findings.

5. Parameter effect and some discussions

In order to analyze the effect of material parameters on the analytical solution, a strengthened beam with size $L \times \varpi \times h = 2300 \times 200 \times 300$ (mm^3) is considered. At the same time, the applied load is taken as P = 100 kN. Fig. 10 to Fig. 15 show the effect of different material parameters on the maximum shear stress and normal stress. It is easily seen in Fig. 10 that the maximum shear stress and normal stress decrease with the increase of elastic modulus of concrete. However, Fig. 11 and Fig. 12 show that both maximum stresses increase with the increase of elastic modulus and thickness of the FRP plate, which indicates that it is not always beneficial in practical engineering to increase the elastic modulus and thickness of the FRP plate.

On the other hand, Fig. 13 to Fig. 15 show that both elastic modulus and shear modulus of the adhesive layer have little influence on the maximum normal stress. At the same time, the elastic modulus of the adhesive layer has very little influence on the maximum shear stress too. But with the increase of the shear modulus or decrease of the thickness of the adhesive layer, the maximum shear stress will increase. In general, the adhesive with small stiffness is desirable in practical engineering. When adhesive is adopted, the interfacial stress can be decreased by increasing the thickness of the adhesive layer to a certain degree. But it is also found that the efficacy of adhesive may be reduced when the adhesive is too thick. So how to choose the thickness of adhesive layer is

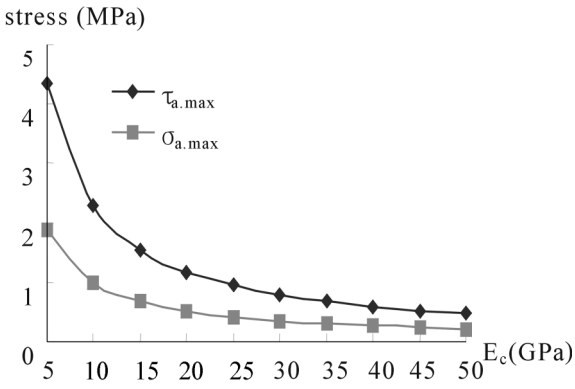

Fig. 10 Influence of E_c on interfacial stress

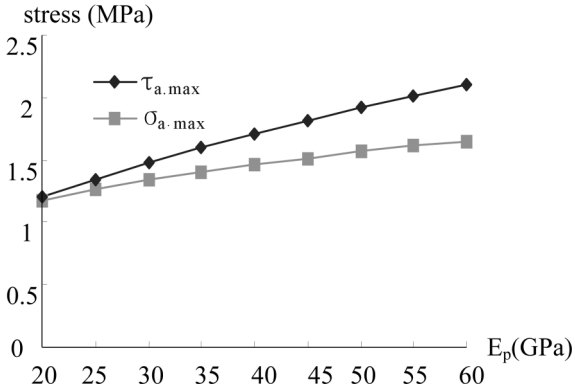

Fig. 11 Influence of E_p on interfacial stress

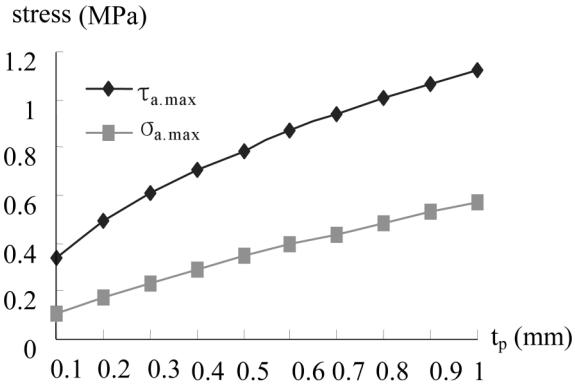

Fig. 12 Influence of t_p on interfacial stress

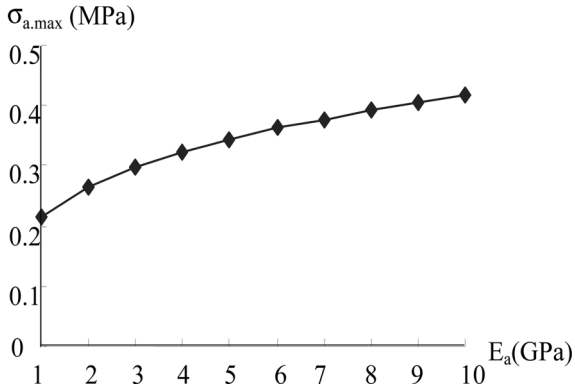

Fig. 13 Influence of E_a on the normal stress

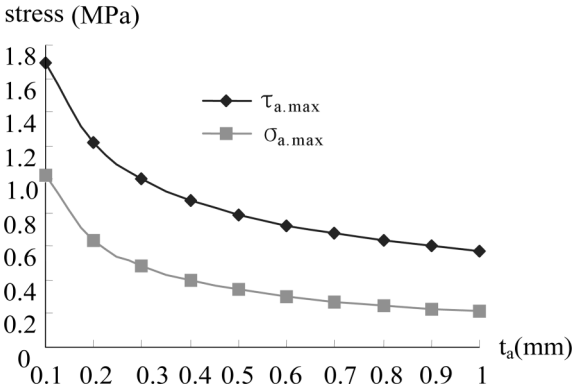

Fig. 14 Influence of t_a on interfacial stress

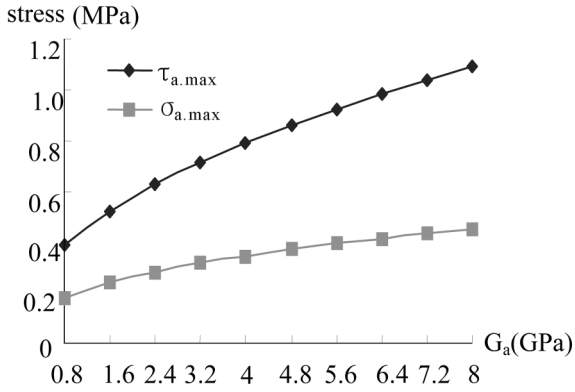

Fig. 15 Influence of G_a on interfacial stress

also needed to be studied especially a lot of engineering practices are needed. It can be easily seen from Fig. 8 and Fig. 9 that with the increase of the value *d*, the shear stress and normal stress at concrete- adhesive interface decrease rapidly. It means that some special treatments such as anchor should be used in the part near the FRP plate's end to avoid interfacial debonding.

6. Conclusions

Based on the theory of elasticity and ignoring some secondary parameters, the present paper provides a theoretical analysis for a four-point bending RC beam strengthened by the FRP plate. The rational simplification taken into the present paper makes both the analytical process and the expressions of formulas concise. The results obtained in the present paper agree well both with the numerical and experimental findings. This research work not only provides a sound background for further investigations of RC beam strengthened by the FRP plate but also is useful for the application of composites in engineering.

Acknowledgements

This research work is financially supported by the National Nature Science Foundation of China (No.50378001). Support is also supplied by the Teaching and Research Award Fund for Outstanding Young Teachers in Higher Education Institutions of MOE, P.R.C.

References

Arduini, M. and Nanni, A. (1997), "Parametric study of beams with externally bonded FRP reinforcement", *ACI Struct. J.*, **94**(5), 493-501.

Arduini, M., Tommas, A.D. and Nanni, A. (1997), "Brittle failure in FRP plate and sheet bonded beams", *ACI Struct. J.*, **94**(4), 363-370.

Chajes, M.J., Finch, W.W., Januszka, T.F. and Thomson, T.A. (1996), "Bond and force transfer of composite material plates bonded to concrete", *ACI Struct. J.*, **93**(2), 259-303.

Malek, A.M., Saadatmanesh, H. and Ehsani, M.R. (1998), "Prediction of failure of R/C beams strengthened with FRP plate due to stress concentration at the plate end", *ACI Struct. J.*, **95**(1), 142-152.

Nakaba, K., Kanakubo, T., Furuta, T. and Yoshizawa, H. (2001), "Bond behavior between fiber-reinforced polymer laminates and concrete", *ACI Struct. J.*, **98**(3), 359-367.

OuYang, Y. and Qian, Z.Z. (2000), "The analysis of bonding shear stress of RC beams strengthened with plate", *China Civil Engineering Journal*, **30**(8), 51-54.

OuYang, Y. and Huang, Y.H. (2002), "Flexural behavior of reinforced concrete beams strengthened with glass fiber", *China Civil Engineering Journal*, **35**(3), 1-8.

Ritchie, P.A., David, A.T., Lu, Le-Wu and Guy, M.C. (1991), "External reinforcement of concrete beams using fiber reinforced plastics", *ACI Struct. J.*, **88**(4), 490-500.

Roberts, T.M. (1989), "Approximate analysis of shear and normal stress concentrations in the adhesive layer of plated RC beams", *Struct. Eng.*, **67**(12), 228-233.

Shahawy, M.A., Arockiasamy, M., Beitelman, T. and Sowrirajan, R. (1996), "Reinforced concrete rectangular beams strengthened with CFRP laminates", *Composite Part B*, **27B**(3/4), 225-233.

Tommaso, A.D., Neubaure, U., Pantuso, A. and Rostasy, F.S. (2001), "Behavior of adhesively bonded concrete-CTRP joints at low and high temperatures", *Mechanics of Composite Materials*, **37**(4), 327-338.

Xie, M., Zhao, L. and Karbhari, V.M. (1995), "Study of bond strength of composites and composite materials", *ICCM-10*, Whistler, B.C., Canada, August, III613-620.

Zheng, D.H. (1999), "Theoretical study and numerical analysis of the mechanical properties of interface in hybrid structures", Master Dissertation of Northern Jiaotong University.

Appendix I

Differentiating Eq. (11) two times and substituting Eq. (1) and Eq. (2) into the obtained equation, we obtain:

$$\begin{cases} \dfrac{d^4 \upsilon_c(x)}{dx^4} = \dfrac{b_p}{E_c I_c}\left[\sigma_a(x) + y_0 \dfrac{d\tau_a(x)}{dx}\right] \\ \dfrac{d^4 \upsilon_p(x)}{dx^4} = \dfrac{b_p}{E_p I_p}\left[\dfrac{d\tau_a(x)}{dx}\dfrac{t_p}{2} - \sigma_a(x)\right] \end{cases} \tag{A}$$

From Eq. (11) and Eq. (A), a differential equation about $\sigma_a(x)$ is obtained

$$\frac{d^4 \sigma_a(x)}{dx^4} + 4\lambda^4 \sigma_a(x) = \gamma \frac{d\tau_a(x)}{dx} \tag{B}$$

where $\lambda^4 = \dfrac{E_a b_p}{4 t_a}\left(\dfrac{1}{E_p I_p} + \dfrac{1}{E_c I_c}\right)$, $\gamma = \dfrac{E_a b_p}{t_a}\left(\dfrac{t_p}{2E_p I_p} - \dfrac{y_0}{E_c I_c}\right)$.

Considering of Eq. (10), Eq. (B) can be rewritten as follows

$$\frac{d^4 \sigma_a(x)}{dx^4} + 4\lambda^4 \sigma_a(x) = -\alpha C_1 \gamma e^{-\alpha x} \tag{C}$$

So the solution of Eq. (11) can be found:

$$\sigma_a(x) = H_1 e^{-\lambda x}\cos(x) + H_2 e^{-\lambda x}\sin(\lambda x) + \sigma_1(x)$$

Notation

The following symbols are used in this paper:

A_c : area of concrete;
A_p : area of FRP plate;
A_s : area of tensile steels;
a : distance between applied load and support;
a_s : thickness of the protective layer of the tensile steels;
$a_{1\text{-}3}$: parameters used in calculating ultimate loads;
a_0 : thickness of the protective layer of the tensile steels;
b_p : width of FRP plate;
$b_{1\text{-}3}$: parameters used in calculating ultimate loads;
C_1 : parameter used in calculating shear stress;
C_2 : parameter used in calculating shear stress;
$c_{1\text{-}3}$: parameters used in calculating ultimate loads
d : distance from FRP plate end to the nearest support;
d_3 : parameters used in calculating ultimate loads;
E_a : elastic modulus of adhesive;
E_c : elastic modulus of concrete;
E_p : elastic modulus of FRP plate;
E_s : elastic modulus of tensile steel;
f_{tk} : tensile strength of concrete;
G_a : shear modulus of adhesive;

H_1 : parameter used in calculating normal stress;
H_2 : parameter used in calculating normal stress;
h : height of beam;
I_c : inertia moment of concrete to its own section;
I_p : inertia moment of FRP plate to its own section;
L : length of beam;
l : length of FRP plate;
M_c : bending moment of concrete;
M_p : bending moment of FRP plate;
N_c : normal tensile force of concrete;
N_p : normal tensile force of FRP plate;
P : applied load of beam;
p : parameter used in calculating ultimate loads;
q : parameter used in calculating ultimate loads;
R_b : vertical reaction load of support;
t_a : thickness of adhesive;
t_p : thickness of FRP plate;
u_c : horizontal displacement of concrete;
u_p : horizontal displacement of FRP plate;
V_c : shear force of concrete;
V_p : shear force of FRP plate;
y_0 : distance between neutral axis of concrete section and x axis;
$\hat{y}_0$: distance between neutral axis of whole section and z axis;
y_c : distance from neutral axis to compression concrete face that strain gets ε_0;
y_p : distance between neutral axis and plate face that strain gets ε_{p0};
α : parameter used in calculating shear stress;
ε_0 : strain of compression concrete when the stress gets σ_{c0};
ε_c : strain of concrete;
ε_{cu} : ultimate strain of compression concrete;
ε_p : strain of FRP plate;
ε_{p0} : strain of FRP plate when the stress gets σ_{py};
ε_{pu} : ultimate strain of FRP plate;
ε_s : strain of tensile steel;
γ : parameter used in calculating normal stress;
η_0 : parameter used in calculating shear stress;
λ : parameter used in calculating normal stress;
ρ : curvature of neutral axis;
σ_a : normal stress of interface between FRP plate and concrete;
$\sigma_{a,\max}$: maximum normal stress of interface between FRP plate and concrete;
σ_c : normal stress of concrete;
σ_{c0} : yield stress of compression concrete;
σ_p : normal stress of FRP plate;
σ_{py} : yield stress of FRP plate;
σ_s : normal stress of tensile steel;
σ_{s0} : yield stress of tensile steel;
σ_1 : maximum principal stress of concrete;
σ_{pu} : ultimate normal stress of FRP plate;
τ_a : shear stress of interface between FRP plate and concrete;
$\tau_{a,\max}$: maximum shear stress of interface between FRP plate and concrete;
υ_c : vertical displacement of concrete;
υ_p : vertical displacement of FRP plate;
ω : width of beam.